

Study of magnetodielectric effect in hexagonal $\text{Ho}_{1-x}\text{Dy}_x\text{MnO}_3$

J. Magesh, P. Murugavel, R. V. K. Mangalam, K. Singh, Ch. Simon, and W. Prellier

Citation: *Journal of Applied Physics* **112**, 104116 (2012); doi: 10.1063/1.4767380

View online: <http://dx.doi.org/10.1063/1.4767380>

View Table of Contents: <http://scitation.aip.org/content/aip/journal/jap/112/10?ver=pdfcov>

Published by the [AIP Publishing](#)

Articles you may be interested in

[Role of rare earth on the \$\text{Mn}^{3+}\$ spin reorientation in multiferroic \$\text{Ho}_{1-x}\text{Lu}_x\text{MnO}_3\$](#)

J. Appl. Phys. **114**, 094102 (2013); 10.1063/1.4819969

[Strong enhancement of magnetoelectric coupling in \$\text{Dy}^{3+}\$ doped \$\text{HoMnO}_3\$](#)

Appl. Phys. Lett. **101**, 022902 (2012); 10.1063/1.4733367

[Large magnetocaloric effect induced by intrinsic structural transition in \$\text{Dy}_{1-x}\text{Ho}_x\text{MnO}_3\$](#)

Appl. Phys. Lett. **100**, 222404 (2012); 10.1063/1.4722930

[Magnetic phase competition in \$\text{Dy}_{1-x}\text{Y}_x\text{MnO}_3\$](#)

J. Appl. Phys. **111**, 07D905 (2012); 10.1063/1.3671795

[Multiferroic properties of \$\text{Bi}_{1-x}\text{Dy}_x\text{FeO}_3\$ nanoparticles](#)

J. Appl. Phys. **106**, 084312 (2009); 10.1063/1.3245390



Study of magnetodielectric effect in hexagonal $\text{Ho}_{1-x}\text{Dy}_x\text{MnO}_3$

J. Magesh,¹ P. Murugavel,^{1,a)} R. V. K. Mangalam,² K. Singh,² Ch. Simon,² and W. Prellier²

¹Department of Physics, Indian Institute of Technology Madras, Chennai 600036, India

²Laboratoire CRISMAT, ENSICAEN/CNRS UMR 6508, 6 Bd Maréchal Juin, 14050 Caen, France

(Received 30 July 2012; accepted 26 October 2012; published online 30 November 2012)

The magnetodielectric studies on hexagonal $\text{Ho}_{1-x}\text{Dy}_x\text{MnO}_3$ reveal an overall enhancement of magnetoelectric coupling upon Dy^{3+} substitution. However, the magnitude of the enhancement is varied with doping level x . Magnetodielectric response is larger for $x=0.1$ and it started decreasing with further increase in x . We suggest that the specific site (C_{3V} site) substitution of higher ionic radii Dy^{3+} in the structure could play a key role in defining magnetoelectric coupling strength through structural distortion. The evolution of c/a ratio which is a measure of distortion in the hexagonal lattice agrees well with the observed percentage change in the dielectric constant which in turn substantiates the role of lattice distortion on the enhancement in magnetodielectric effect. © 2012 American Institute of Physics. [<http://dx.doi.org/10.1063/1.4767380>]

I. INTRODUCTION

Multiferroics are a class of materials which exhibit several ferroic orders simultaneously, i.e., they are ferroelectric, ferromagnetic, and ferroelastic.¹⁻³ The inherent magnetoelectric coupling of these materials entail them for potential applications as they offer an additional degree of freedom in device design.^{4,5} Even though the existence of such magnetoelectric coupling has been predicted long back, their observation is limited,⁶ as their origin is mutually exclusive in conventional materials.⁷ However, the magnetoelectric coupling is observed recently in several new class of compounds where the origin is different from that of conventional ferroelectric and ferromagnetic materials.⁸ Rare earth hexagonal manganites RMnO_3 ($R = \text{Y}, \text{Ho}, \text{Er}, \text{Tm}, \text{Yb}, \text{and Lu}$)⁹ is an important class of such multiferroic material in which the ferroelectricity around 900 K is attributed to the buckling of MnO_5 polyhedra, whereas the magnetism is ascribed to planar 120° triangular antiferromagnetic ordering of Mn^{3+} in the a - b plane at 70 K (T_N).^{10,11} The observation of dielectric anomalies at the magnetic ordering temperatures corroborates the magnetoelectric coupling in these compounds.¹²⁻¹⁴ Even though the very low dielectric loss of RMnO_3 makes them preferential for practical application, its distinct advantage pales in front of their shortcomings, namely, low magnetic ordering temperatures and the weak magnetoelectric coupling.¹⁵ But, much to the dismay, most of the studies of RMnO_3 are concentrated on magnetic phase transitions, whereas the magnetoelectric coupling study is ignored. The aim of our study is to explore and enhance the magnetoelectric strength of such materials. A weak magnetoelectric coupling is predicted in hexagonal RMnO_3 as the axis of polarization (c direction)¹⁶ and the axis of magnetization (along the ab -plane)¹⁷ are non-interactive in nature. However, a strong magnetoelectric coupling can be achieved if, either the magnetization has component along the c axis or polarization has a component along a or b axis.

Of this RMnO_3 family, HoMnO_3 which is at the end of the hexagonal phase boundary has a rich magnetic phase diagram.¹⁸⁻²⁰ The slight higher ionic radii Dy^{3+} crystallize in an entirely different orthorhombic phase of RMnO_3 at ambient pressure and temperature.^{21,22} Dy^{3+} which is at the phase boundary between the hexagonal and orthorhombic phases, upon substitution in HoMnO_3 , could lead to a strong lattice distortion in the hexagonal lattice which in turn is expected to strengthen the magnetoelectric coupling. Our recent report on $\text{Ho}_{0.9}\text{Dy}_{0.1}\text{MnO}_3$ compound confirms the expected enhancement in magnetoelectric coupling.²³ Interestingly, in parent HoMnO_3 , $1/3^{\text{rd}}$ of Ho^{3+} ion occupies C_{3V} site and remaining $2/3^{\text{rd}}$ occupies C_3 site.²⁴ We believe that upon doping, the dopant is expected to occupy either C_{3V} or C_3 site depending on its ionic radii which will in turn could affect the behavior of structural distortion and hence the magnetoelectric coupling. In order to study the evolution of magnetoelectric coupling on Dy^{3+} substituted HoMnO_3 , we synthesized $\text{Ho}_{1-x}\text{Dy}_x\text{MnO}_3$ ($x = 0, 0.1, 0.2, \text{and } 0.3$) polycrystalline samples and studied their magnetodielectric effect. The results strongly indicate the correlation between the lattice distortion, site specific substitution, and magnetoelectric coupling.

II. EXPERIMENTAL

Conventional solid state synthesis technique is employed in order to prepare polycrystalline hexagonal $\text{Ho}_{1-x}\text{Dy}_x\text{MnO}_3$ ($x = 0, 0.1, 0.2, \text{and } 0.3$) compounds. In the first phases, the parent compounds HoMnO_3 and DyMnO_3 are synthesized from stoichiometric amount of Ho_2O_3 , Mn_2O_3 , and Dy_2O_3 . The stoichiometric proportion of the parent compounds is then ground well and calcinated at 1350°C for 12h for several times to get uniform composition. Powder x-ray diffraction (XRD) patterns are obtained for the polycrystalline $\text{Ho}_{1-x}\text{Dy}_x\text{MnO}_3$ ($x = 0, 0.1, 0.2, \text{and } 0.3$) using a PANalytic x-ray diffractometer. Agilent 4248 RLC bridge integrated to Physical Property Measurement System (PPMS) is employed to measure the capacitance at 100 kHz. PPMS is utilized in order to maintain the temperature at 10 K and vary the magnetic field from 0 to 14 T.

^{a)}Electronic mail: muruga@iitm.ac.in.

III. RESULTS AND DISCUSSION

A. Crystal structure

The x-ray diffraction patterns obtained for the $\text{Ho}_{1-x}\text{Dy}_x\text{MnO}_3$ ($x=0, 0.1, 0.2,$ and 0.3) compounds are shown in Figure 1. The obtained patterns confirm that all the synthesized compounds are crystallized in hexagonal structure with $P6_3\text{cm}$ space group without any trace of the competing orthorhombic phase. The lattice parameters obtained are increasing with the increase in Dy^{3+} content. The c/a ratio attains the maximum value of 1.8585 for $x=0.1$ and decreases thereafter as shown in the inset of Figure 1. The obtained c/a ratio is 1.8583 for $x=0.2$ which is less than that of $x=0.1$ compound but higher than that of pure HoMnO_3 ($c/a=1.8581$). On further increase of Dy^{3+} content, the c/a ratio shows downward trend.

B. Magnetodielectric response

In order to study the magnetoelectric coupling of polycrystalline $\text{Ho}_{1-x}\text{Dy}_x\text{MnO}_3$ ($x=0, 0.1, 0.2,$ and 0.3) samples, the dielectric constant (ϵ_r) is measured as a function of the magnetic field from 0 to 14 T in both positive and negative directions. A complete ϵ_r vs. magnetic field loop is traced in order to study the reversibility of the magnetoelectric coupling. The magnetoelectric coupling strength is measured as percentage change in dielectric constant with applied field as defined by $\% \Delta \epsilon_r = \left[\frac{\epsilon_r(H) - \epsilon_r(H=0)}{\epsilon_r(H=0)} \right] \times 100$. According to the phase diagram of Lorenz,¹⁸ the single crystalline HoMnO_3 should exhibit three magnetic phases in the region of study. They are $P6_3'c'm$, $P6_3'$, and $P6_3\text{cm}$ exist in the field range of 0 to 2.5 T, 2.5 to 3.5 T, and above 3.5 T, respectively. But, the existence of these phases is not apparently visible in the magnetodielectric response of polycrystalline pure HoMnO_3 .²³ This may be due to the weak magnetoelectric coupling in HoMnO_3 (maximum observed $\% \Delta \epsilon_r$ is only 0.08% at 10 K) and it agrees well with that of YbMnO_3 in shape and magnitude.²⁵ Incidentally on Dy^{3+} substitution, the magnetodielectric study not only reveals the signature of

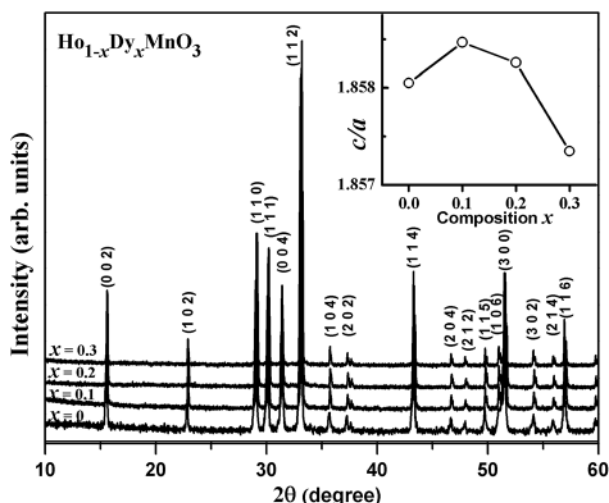


FIG. 1. XRD patterns of polycrystalline $\text{Ho}_{1-x}\text{Dy}_x\text{MnO}_3$ ($x=0, 0.1, 0.2,$ and 0.3). Inset shows the variation of c/a ratio with x .

various magnetic phases but also shows enhancement in magnetodielectric effect by more than an order of magnitude. Note that the dielectric loss below 100 K is observed to be of the order of 0.002 indicating typical dielectric characteristics of our samples. Hence, the contribution from the magnetoresistance to the dielectric response if any can be neglected.

The Dy^{3+} substitution in HoMnO_3 leads to a complex magnetodielectric response due to various competing magnetic interactions. Figure 2 shows the variation of dielectric constant as a function of magnetic field for $\text{Ho}_{0.9}\text{Dy}_{0.1}\text{MnO}_3$ at 10 K. The magnetodielectric response observed in $\text{Ho}_{0.9}\text{Dy}_{0.1}\text{MnO}_3$ shows a well demarcated boundary at the reported magnetic phase transitions which is in line with the magnetic phase diagram of HoMnO_3 .²⁴ Accordingly, the magnetodielectric response observed in $\text{Ho}_{0.9}\text{Dy}_{0.1}\text{MnO}_3$ is divided into three regions marked as I, II, and III in Figure 2. The region I has a contribution from $P6_3'c'm$ phase extending up to a magnetic field of 2.4 T. The region II has a contribution from the intermediate phase $P6_3'$ which extends up to a magnetic field of 4.5 T. The region III is due to the high temperature magnetic phase $P6_3\text{cm}$.

In the region I, on increasing the magnetic field from 0 to 2.5 T, the dielectric constant remains constant but upon decreasing the field, an open loop behavior is observed. The region II also shows an open loop behavior from 2.5 to 4.8 T. During the positive sweep (solid triangle in Fig. 2), the dielectric constant raises and falls sharply around 3 T, whereas during the reverse sweep (open circles in Fig. 2) it remains constant. In region III, the dielectric constant drops sharply at 9 T and on decreasing the field it reaches the maximum at 4.8 T. The magnetodielectric response displays a symmetric behavior upon switching the field in negative direction which can be correlated to the inherent response of various magnetic phases mentioned earlier. The $\text{Ho}_{0.9}\text{Dy}_{0.1}\text{MnO}_3$ shows 2.5% change in dielectric constant compared to 0.08% change

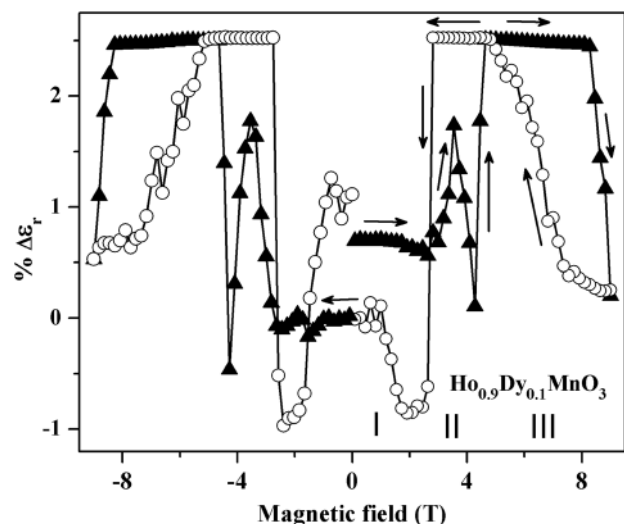


FIG. 2. Percentage change of the dielectric constant as a function of applied magnetic field for $\text{Ho}_{0.9}\text{Dy}_{0.1}\text{MnO}_3$. The solid triangles and open circles represent the increase and decrease in magnitude of field, respectively. Reprinted with permission from Magesh *et al.*, Appl. Phys. Lett. **101**, 022902 (2012). Copyright 2012 American Institute of Physics.

observed in parent HoMnO_3 compound. Such a strong enhancement (32 times) is attributed to lattice frustration arises from the higher ionic radii Dy^{3+} substitution.

Figure 3 shows the variation of dielectric constant as a function of applied magnetic field for $\text{Ho}_{0.8}\text{Dy}_{0.2}\text{MnO}_3$ at 10 K. On increasing the dopant Dy^{3+} concentration to $x=0.2$, the $\% \Delta \epsilon_r$ drops down to 1.6% which is half the value as that of $\text{Ho}_{0.9}\text{Dy}_{0.1}\text{MnO}_3$ but still large (20 times) compared to the parent HoMnO_3 compound. The region I extends to 3.2 T in the positive field side, whereas it extends to 4.2 T in the negative field side. Region I shows a partial open loop behavior, but the region II shows open loop behavior. Interestingly, in region III, the open loop behavior is vanished in comparison to larger open loop behavior observed in $\text{Ho}_{0.9}\text{Dy}_{0.1}\text{MnO}_3$.

Figure 4 shows the $\% \Delta \epsilon_r$ as a function of applied magnetic field for $\text{Ho}_{0.7}\text{Dy}_{0.3}\text{MnO}_3$ measured at 10 K. $\text{Ho}_{0.7}\text{Dy}_{0.3}\text{MnO}_3$ shows only 0.13% change in dielectric constant which is still larger (almost double) compared to HoMnO_3 but smaller compared to $x=0.1$ and 0.2 compounds. All the three regions I, II, and III show a slight open loop behavior. Even though the phase boundary is not accompanied by sharp changes in the dielectric constants as that of $\text{Ho}_{0.9}\text{Dy}_{0.1}\text{MnO}_3$ and $\text{Ho}_{0.8}\text{Dy}_{0.2}\text{MnO}_3$, but they can be demarcated from the change in the slope of dielectric constant. Regions I, II, and III extend up to a magnetic field of 3.2, 4.8, and above 4.8 T, respectively.

C. Site specific substitution and structural distortion

Overall, the $\% \Delta \epsilon_r$ increases drastically from 0.08% for HoMnO_3 to 2.5% for $\text{Ho}_{0.9}\text{Dy}_{0.1}\text{MnO}_3$. On further increase in Dy content, $\% \Delta \epsilon_r$ decreases to 1.6% for $\text{Ho}_{0.8}\text{Dy}_{0.2}\text{MnO}_3$ and 0.13% for $\text{Ho}_{0.7}\text{Dy}_{0.3}\text{MnO}_3$ which is similar in magnitude as that of HoMnO_3 . The variation of magnetodielectric response with the increase in Dy^{3+} substitution can be explained on the basis of site specific substitution. The Ho^{3+} occupies two different sites, namely, C_{3V} and C_3 in hexagonal HoMnO_3 structure. The C_{3V} site present at the

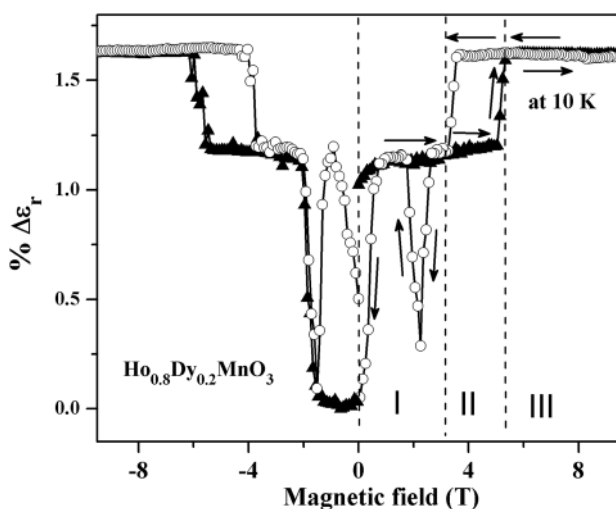


FIG. 3. Percentage change of the dielectric constant as a function of applied magnetic field for $\text{Ho}_{0.8}\text{Dy}_{0.2}\text{MnO}_3$. The solid triangles and open circles represent the increase and decrease in magnitude of field, respectively.

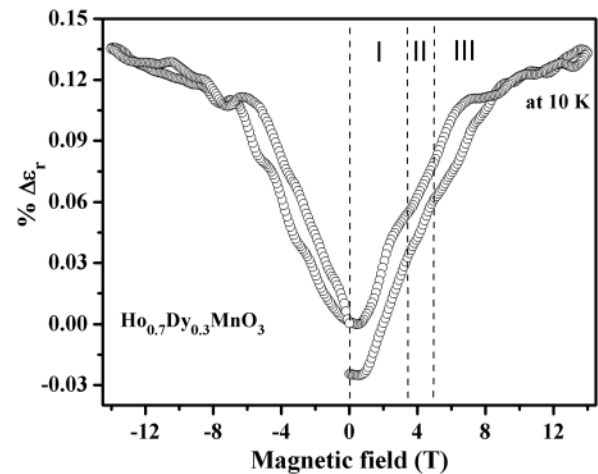


FIG. 4. Percentage change of the dielectric constant as a function of applied magnetic field for $\text{Ho}_{0.7}\text{Dy}_{0.3}\text{MnO}_3$.

edge of the unit cell (with positional coordinates as $(0, 0, 1/4 - \delta)$) is occupied by $1/3^{\text{rd}}$ of the Ho^{3+} which holds the unit cell together. On the other hand, the C_3 site present well inside the unit cell (with positional coordinates as $(1/3, 2/3, 1/4 + \delta)$) is occupied by $2/3^{\text{rd}}$ Ho^{3+} which decides the inter layer separation of Mn^{3+} . Van Aken *et al.* observed a sudden change of lattice parameter on Zr^{4+} substitution of YMnO_3 which can be due the site specific substitution.²⁶ Zhou *et al.* reported an increase in the strength of the magnetic transition at 5 K on substituting the non-magnetic Y^{3+} .²⁷ The transition at 5 K is attributed to Ho^{3+} ordering. The increase in strength of the magnetic transition upon non-magnetic substitution also gives the clue about the site specific substitution of Y^{3+} at the C_3 site. The spin reorientation vanishes at $2/3^{\text{rd}}$ in Y^{3+} also indicates the site specific substitution. On the similar line, we expect the higher ionic radii Dy^{3+} prefer the more symmetric C_{3V} site. Upon Dy^{3+} substitution, when $x=0.1$, the Dy^{3+} can preferably occupies the C_{3V} site by replacing one of the four Ho^{3+} which holds the unit cell thus effectively leads to a maximum distortion. When $x=0.2$, slightly more than half of the Ho^{3+} in C_{3V} site can be replaced by Dy^{3+} and thereby reducing the amount of distortion due to the balance between Ho^{3+} and Dy^{3+} ions in the C_{3V} site which is responsible for the decrease in magnetoelectric coupling. At $x=0.3$, the Ho^{3+} at C_{3V} site is almost replaced by the Dy^{3+} thus forming a stable structure thereby effectively suppressing the structural distortion. This is very well reflected in the low magnetodielectric response observed for $\text{Ho}_{0.7}\text{Dy}_{0.3}\text{MnO}_3$ compound which has similar characteristics shown by the parent HoMnO_3 compound. The measured magnetodielectric response for $\text{Ho}_{1-x}\text{Dy}_x\text{MnO}_3$ supports our proposed site specific dopant substitution in the compound.

Since the c/a ratio is a measure of lattice distortion, we expected that the variation in distortion upon Dy^{3+} substitution could very well be reflected in the c/a ratio. As expected, the c/a ratio reaches a maximum for the compound $x=0.1$ confirming the large distortion in the structure due to doping. Accordingly, our dielectric constant measurements also revealed maximum $\% \Delta \epsilon_r$ for this compound. On further

increase in dopant concentration, for $x=0.2$, the c/a ratio shows decreasing trend. The decrease in c/a ratio for $x=0.2$ compound could be due to the partial suppression of distortion by Dy^{3+} substitution which is indeed reflected in $\% \Delta \epsilon_r$. The almost suppression of distortion upon $1/3^{\text{rd}}$ doping is evident for $x=0.3$ compound from its decrease in $\% \Delta \epsilon_r$ and c/a ratio values.

IV. CONCLUSION

In conclusion, the magnetodielectric studies on $\text{Ho}_{1-x}\text{Dy}_x\text{MnO}_3$ compound revealed the existence of complex magnetic phases at different magnetic fields. The magnetodielectric effect is enhanced strongly on Dy^{3+} substitution in HoMnO_3 . We observed 2.5%, 1.6%, and 0.13% maximum change in magnetodielectric effect for $\text{Ho}_{0.9}\text{Dy}_{0.1}\text{MnO}_3$, $\text{Ho}_{0.8}\text{Dy}_{0.2}\text{MnO}_3$, and $\text{Ho}_{0.7}\text{Dy}_{0.3}\text{MnO}_3$, respectively, compared to 0.08% in magnetodielectric effect for the HoMnO_3 . We strongly believe that the site specific (C_{3V} site) substitution of Dy^{3+} at Ho^{3+} in HoMnO_3 and the resultant lattice distortion could explain the change in magnitude of magnetodielectric effect in $\text{Ho}_{1-x}\text{Dy}_x\text{MnO}_3$. The attribution of lattice distortion to the observed magnetodielectric response is corroborated by the change in c/a ratio which is the measure of distortion in the hexagonal lattice.

ACKNOWLEDGMENTS

Dielectric measurement is done in the frame of the Laboratoire Franco-Indien pour la Cooperation Scientifique (LAFICS).

¹N. A. Hill, *J. Phys. Chem. B* **104**, 6694 (2000).

²W. Prellier, M. P. Singh, and P. Murugavel, *J. Phys.: Condens. Matter* **17**, R803 (2005).

³D. I. Khomskii, *J. Magn. Magn. Mater.* **306**, 1 (2006).

⁴Y. H. Chu, L. W. Martin, M. B. Halcomb, and R. Ramesh, *Mater. Today* **10**, 16 (2007).

⁵Th. Lottermoser, T. Lonkai, U. Amann, D. Hohlwein, J. Ihringer, and M. Fiebig, *Nature* **430**, 541 (2004).

⁶D. N. Astrov, *Sov. Phys. JETP* **11**, 708 (1960).

⁷S.-W. Cheong and M. Mostovoy, *Nature Mater.* **6**, 13 (2007).

⁸R. Ramesh, *Nature* **461**, 1218 (2009).

⁹G. A. Smolenskii and V. A. Bokov, *J. Appl. Phys.* **35**, 915 (1964).

¹⁰K. Lukaszewicz and J. Karut-Kalicinska, *Ferroelectrics* **7**, 81 (1974).

¹¹W. C. Koehler, H. L. Yakel, E. O. Wollan, and J. W. Cable, *Phys. Lett.* **9**, 93 (1964).

¹²Z. J. Huang, Y. Cao, Y. Y. Sun, Y. Y. Xue, and C. W. Chu, *Phys. Rev. B* **56**, 2623 (1997).

¹³T. Katsufuji, M. Masaki, A. Machida, M. Moritomo, K. Kato, E. Nishibori, M. Takata, M. Sakata, K. Ohoyama, K. Kitazawa, and H. Takagi, *Phys. Rev. B* **66**, 134434 (2002).

¹⁴D. G. Tomuta, S. Ramakrishnan, G. J. Nieuwenhuys, and J. A. Mydosh, *J. Phys.: Condens. Matter* **13**, 4543 (2001).

¹⁵P. Coeure, P. Guinet, J. C. Peuzin, G. Buisson, and E. F. Bertaut, in *Proceedings of International Meeting on Ferroelectricity* (1966), Vol. 1, p. 332.

¹⁶B. B. Van Aken, T. M. Palstra, A. Filippetti, and N. A. Spaldin, *Nature Mater.* **3**, 164 (2004).

¹⁷Th. Lonkai, D. G. Tomuta, J.-U. Hoffmann, R. Schneider, D. Hohlwein, and J. Ihringer, *J. Appl. Phys.* **93**, 8191 (2003).

¹⁸B. Lorenz, F. Yen, M. M. Gospodinov, and C. W. Chu, *Phys. Rev. B* **71**, 014438 (2005).

¹⁹M. Fiebig, C. Degenhardt, and R. V. Pisarev, *J. Appl. Phys.* **91**, 8867 (2002).

²⁰P. Murugavel, J. H. Lee, D. Lee, T. W. Noh, Y. H. Jo, M. W. Jung, Y. S. Oh, and K. H. Kim, *Appl. Phys. Lett.* **90**, 142902 (2007).

²¹J. H. Lee, P. Murugavel, D. Lee, T. W. Noh, Y. Jo, M. H. Jung, K. H. Jang, and J.-G. Park, *Appl. Phys. Lett.* **90**, 012903 (2007).

²²S. Harikrishnan, S. Rößler, C. M. Naveen Kumar, H. L. Bhat, U. K. Rößler, S. Wirth, F. Steglich, and Suja Elizabeth, *J. Phys.: Condens. Matter* **21**, 096002 (2009).

²³J. Magesh, P. Murugavel, R. V. K. Mangalam, K. Singh, Ch. Simon, and W. Prellier, *Appl. Phys. Lett.* **101**, 022902 (2012).

²⁴N. Abramov, V. Chichkov, S. E. Lofland, and Y. M. Mukovskii, *J. Appl. Phys.* **109**, 07D912 (2011).

²⁵H. Sugie, N. Iwata, and K. Kohn, *J. Phys. Soc. Jpn.* **71**, 1558 (2002).

²⁶B. B. Van Aken, J. -W. G. Bos, R. A. de Groot, and T. T. M. Palstra, *Phys. Rev. B* **63**, 125127 (2001).

²⁷H. D. Zhou, J. Lu, R. Vasic, B. W. Vogt, J. A. Janik, S. Brooks, and C. R. Wiebe, *Phys. Rev. B* **75**, 132406 (2007).